ORIGINAL ARTICLE

Phenotypes of CCAAT/enhancer-binding protein beta deficiency: hyperdontia and elongated coronoid process

B Huang[1,2], K Takahashi[2], T Sakata-Goto[2], H Kiso[2], Y Togo[2], K Saito[2], H Tsukamoto[2], M Sugai[3], S Akira[4], A Shimizu[3], K Bessho[2]

[1]Department of Paediatric Dentistry, School of Medicine and Dentistry, James Cook University, Cairns, Australia; [2]Department of Oral and Maxillofacial Surgery, Graduate School of Medicine, Kyoto University, Kyoto, Japan; [3]Translational Research Center, Kyoto University Hospital, Kyoto University, Kyoto, Japan; [4]Laboratory of Host Defense, World Premier International Immunology Frontier Research Center, Osaka University, Osaka, Japan

OBJECTIVES: This investigation aimed to conduct a case–control study of mandibular morphology and dental anomalies to propose a relationship between mandibular/dental phenotypes and deficiency of CCAAT/enhancer-binding protein beta (CEBPB).

MATERIALS AND METHODS: Skulls of CEBPB$^{-/-}$, CEBPB$^{+/-}$ and CEBPB$^{+/+}$ mice were inspected with micro-computed tomography. Mandibular morphology was assessed with a method of Euclidean distance matrix analysis.

RESULTS: Elongation of the coronoid process was identified in CEBPB$^{+/-}$ ($P \leq 0.046$) and CEBPB$^{-/-}$ 12-month-olds ($P \leq 0.028$) but not in 14-day-olds ($P \geq 0.217$) and 0-day-olds ($P \geq 0.189$) of either genotype. Formation of supernumerary teeth in CEBPB$^{-/-}$ adult mice was demonstrated ($\chi^2 = 6.00$, df = 1, $P = 0.014$).

CONCLUSIONS: CEBPB deficiency was related to elongation of the coronoid process and formation of supernumerary teeth. The mandibular and dental phenotypes of CEBPB deficiency were unseen by the 14th day after birth. Future investigations into the influence of CEBPB on mandibular and dental development are needed.
Oral Diseases (2012) doi: 10.1111/j.1601-0825.2012.01963.x

Introduction

CCAAT/enhancer-binding protein beta (CEBPB, also known as C/EBP β and NF-IL6) is a transcription factor, which binds to consensus sequences and affects the transcription of various genes involved in proliferation and differentiation, such as cells in the mammary gland (Seagroves *et al*, 1998) and the immune system (Tanaka *et al*, 1995; Poli, 1998). This gene has been mapped to human chromosome 20 (Hendricks-Taylor *et al*, 1992). In addition to the above relevance, previous studies have suggested CEBPB as a key factor in osteogenesis, chondrogenesis and odontogenesis (McCarthy *et al*, 2000; Gutierrez *et al*, 2002; Narayanan *et al*, 2004; Harrison *et al*, 2005; Savage *et al*, 2006; Wiper-Bergeron *et al*, 2007; Tominaga *et al*, 2008; Hirata *et al*, 2009).

During ossification, CEBPB is implicated in the regulation of insulin-like growth factor 1 (IGF1) (McCarthy *et al*, 2000), runt-related transcription factor 2 (RUNX2, also known as CBFA1) (Gutierrez *et al*, 2002; Wiper-Bergeron *et al*, 2007), bone gamma-carboxyglutamate (gla) protein (BGLAP, also known as osteocalcin) (Gutierrez *et al*, 2002) and cyclin-dependent kinase inhibitor 1C (CDKN1C, also known as p57^{Kip2}) (Hirata *et al*, 2009). With such a significance, a relationship between delayed bone formation and impaired CEBPB function has been established (Harrison *et al*, 2005; Savage *et al*, 2006; Wiper-Bergeron *et al*, 2007; Tominaga *et al*, 2008; Hirata *et al*, 2009). Reported consequences of CEBPB homozygous deficiency included suppressed differentiation of osteoblasts, restrained hypertrophy of chondrocytes and retarded maturation in both types of cells (Tominaga *et al*, 2008; Hirata *et al*, 2009). Furthermore, overexpression of p20CEBPB (also known as LIP), a dominant negative CEBPB isoform, was responsible for inhibition of terminal osteoblast differentiation in transgenic mice (Harrison *et al*, 2005; Savage *et al*, 2006). This in turn contributed to a reduced amount of alveolar bone and a lower bone volume fraction of the mandible (Savage *et al*, 2006). On the other hand, repression of chondrocyte proliferation, suppression of early osteoblast differentiation and enhancement of chondrocyte

hypertrophy were induced by overexpression of CEBPB (Wiper-Bergeron *et al*, 2007; Hirata *et al*, 2009).

A previous study has demonstrated CEBPB repressed manifestation of the dentine sialophosphoprotein (DSPP) gene during odontoblast differentiation (Narayanan *et al*, 2004). Dentinogenesis imperfecta, a hereditary tooth defect, has been observed in humans with a mutant DSPP gene (Kim *et al*, 2005) and in p20CEBPB transgenic mice (Savage *et al*, 2006). Of further note, earlier studies have suggested an influence of IGF1 on dental maturation (Campbell *et al*, 2009), a preventing effect of RUNX2 upon development of succedaneous tooth organs (D'Souza *et al*, 1999), and an odontogenic relevance of BGLAP (Salmela *et al*, 2012). As mentioned earlier, activity of IGF1, RUNX2 and BGLAP was subject to CEBPB regulation (McCarthy *et al*, 2000; Gutierrez *et al*, 2002; Wiper-Bergeron *et al*, 2007). Thus, involvement of CEBPB in odontogenesis via interactions with DSPP, IGF1, RUNX2 and/or BGLAP is conjectured.

Although a past study has described dental and mandibular defects of p20CEBPB transgenic mice (Savage *et al*, 2006), mandibular and dental phenotypes of mice with CEBPB deficiency have never been reported. This investigation aimed, therefore, to conduct a case–control study of mandibular morphology and dental anomalies, using a sample of $CEBPB^{-/-}$, $CEBPB^{+/-}$ and $CEBPB^{+/+}$ mice. A special interest was to propose a relationship of mandibular/dental phenotypes to CEBPB homozygous and heterozygous deficiency.

Materials and methods

Prior to commencement, this study has received appropriate ethics approval from the Animal Research Committee of Kyoto University (Reference Number: Med Kyo 11518). $CEBPB^{+/-}$ and $CEBPB^{-/-}$ mice were generated as described previously (Tanaka *et al*, 1995). Seventy-one female mice of a CEBPB/129-Ter strain were euthanised with carbon dioxide gas for investigation. These included 12 $CEBPB^{-/-}$ (five 0-day-olds, one 14 day old and six 12-month-olds), 37 $CEBPB^{+/-}$ (eleven 0-day-olds, sixteen 14-day-olds and ten 12-month-olds) and 22 $CEBPB^{+/+}$ (seven 0-day-olds, nine 14-day-olds and six 12-month-olds) mice. All of the 0-day-old and 14-day-old female pups separately born in seven and nine litters were selected. Owing to a high neonatal mortality of $CEBPB^{-/-}$ mice (Bai *et al*, 2006), only one 14 day old of this genotype was attainable in the sample. Consequently, quantitative analysis for 14-day-olds was merely made between $CEBPB^{+/-}$ and $CEBPB^{+/+}$ pups. Of further note, sex of 0-day-olds was determined according to anogenital pigmentation (Wolterink-Donselaar *et al*, 2009). A pilot experiment has been carried out by comparing the observed anogenital pigmentation at birth with the genital appearance at 3 months of age amongst 10 randomly selected pups. Outcomes of the pilot experiment indicated 100% reliability of the sex establishing method used for this strain.

Upon killing, murine skulls were assessed with a micro-computed tomography (micro-CT) scanner (SMX-100CT-SV3; Shimadzu, Kyoto, Japan). The micro-CT technique was applied to identify predetermined mandibular landmarks (Cook, 1965; Richtsmeier *et al*, 2000) and to examine prospective dental anomalies including hypodontia as well as supernumerary teeth. Three-dimensional linear distances between the identifiable landmarks were measured using a method of Euclidean distance matrix analysis (EDMA) (Lele, 1993). As mice have an unfused expandable mandibular symphysis (Barbosa *et al*, 2007), EDMA linear distances between the two halves of the mandible were not assessed by this study.

To identify the expression of CEBPB, mRNA expression of the target gene was examined. Tissues used for this purpose were collected from the coronoid process, the condyle and the mandibular angle of a $CEBPB^{+/+}$ adult mouse. Procedures for preparation of the reverse transcriptase polymerase chain reaction (RT-PCR), as suggested by previous studies (Harrison *et al*, 2005; Kawagishi *et al*, 2008), were carried out. Amplification was performed with employment of Ex Taq polymerase (TaKaRa, Tokyo, Japan) and specific primers for murine CEBPB (sense primer, 5′-ACACGTGTAACTG TCAGCCG-3′; antisense primer, 5′-GCTCGAAACG-GAAAAGGTTC-3′) (Kawagishi *et al*, 2008). This was initiated with denaturation (30 s, 94°C), followed by annealing (30 s, 59°C) and extension (30 s, 72°C), for 30 cycles in a GeneAmp PCR System 9700 thermal cycler (Applied Biosystems, Foster City, CA, USA). Specific primers for murine glyceraldehyde-3-phosphate dehydrogenase (GAPDH) were used to check the internal control (Suzuki *et al*, 2000). All procedures were carried out according to the manufacturers' instructions.

Data entry and statistical analysis were conducted with the IBM SPSS Statistics (version 19.0; IBM Corporation, Somers, NY, USA). Data analysis included descriptive statistics (frequency distribution and cross-tabulation). An independent samples *t*-test method was used to assess the difference in the EDMA linear distances between CEBPB deficient cases ($CEBPB^{+/-}$ or $CEBPB^{-/-}$ mice) and the controls ($CEBPB^{+/+}$ mice) (Altman, 1990). To test the relationship between occurrence of dental anomalies and genotypes of CEBPB, a Pearson's chi-square test was carried out (Altman, 1990). The level of two-sided significance was set at 5%.

Results

Compared with $CEBPB^{+/+}$ adult mice (df = 14), $CEBPB^{+/-}$ 12-month-olds showed a larger EDMA linear distance from Landmark 1 (coronoid process) to Landmark 2 (mandibular angle) ($t = -2.26$, $P = 0.040$), to Landmark 7 (superior-most point on inferior border of mandibular ramus) ($t = -3.68$, $P = 0.002$), to Landmark 8 (inferior-most point on border of ramus inferior to incisor alveolar) ($t = -2.19$, $P = 0.046$), to Landmark 9 (inferior-most point on incisor alveolar rim) ($t = -3.22$, $P = 0.006$), to Landmark 10

(superior-most point on incisor alveolar rim) ($t = -3.56$, $P = 0.003$), to Landmark 11 (mental foramen) ($t = -3.45$, $P = 0.004$), to Landmark 12 (anterior point on molar alveolar rim) ($t = -3.06$, $P = 0.008$) as well as to Landmark 13 (intersection of molar alveolar rim and base of coronoid process) ($t = -2.92$, $P = 0.011$), from Landmark 6 (posterior-most point on mandibular condyle) to Landmark 7 ($t = -2.34$, $P = 0.034$), from L8 to L9 ($t = -3.07$, $P = 0.008$), to Landmark 10 ($t = -2.84$, $P = 0.018$), to Landmark 11 ($t = -3.02$, $P = 0.009$) as well as to Landmark 12 ($t = -3.99$, $P = 0.003$), and from Landmark 10 to Landmark 12 ($t = -2.18$, $P = 0.047$) (Fig. 1a,d) (Table 1). Based on the above, eight (88.9%) of the nine EDMA line segments ending at the coronoid process were longer amongst CEBPB$^{+/-}$ adults than the controls.

Similarly, CEBPB$^{-/-}$ adults displayed a larger EDMA linear distance from Landmark 1 to Landmark 7 ($t = -2.63$, $P = 0.025$), to Landmark 12 ($t = -2.72$, $P = 0.021$) as well as to Landmark 13 ($t = -2.56$, $P = 0.028$), and from Landmark 8 to Landmark 11 ($t = -2.80$, $P = 0.019$) as well as to Landmark 12 ($t = -2.80$, $P = 0.019$) than CEBPB$^{+/+}$ mice (df = 10) (Fig. 1b,d) (Table 2). These indicated that three (33.3%) of the nine EDMA line segments originating

from the coronoid process were longer in CEBPB$^{-/-}$ adults compared with the controls.

When comparing CEBPB$^{-/-}$ with CEBPB$^{+/-}$ adults (df = 14), the former exhibited a smaller EDMA linear distance from Landmark 1 to Landmark 2 ($t = 3.42$, $P = 0.004$) as well as to Landmark 6 ($t = 2.43$, $P = 0.029$), from Landmark 2 to Landmark 6 ($t = 3.14$, $P = 0.007$) as well as to Landmark 13 ($t = 2.24$, $P = 0.042$), from Landmark 6 to Landmark 12 ($t = 2.22$, $P = 0.044$), and from Landmark 8 to Landmark 9 ($t = 2.56$, $P = 0.023$) (Fig. 1c,d) (Table 3). The most distinguishable anatomical landmarks between the two CEBPB deficient genotypes included the condyle (three of the nine EDMA line segments), the mandibular angle (three of the nine EDMA line segments) and the coronoid process (two of the nine EDMA line segments). Furthermore, EDMA linear distances related to the coronoid process did not differ among CEBPB$^{-/-}$, CEBPB$^{+/-}$ and CEBPB$^{+/+}$ pups at the age of 0 day ($P \geq 0.189$) and 14 days ($P \geq 0.217$), respectively. There was also no difference in the linear distances originating from other portions of the mandible among any genotypes in 0-day-olds ($P \geq 0.139$) and 14-day-olds ($P \geq 0.086$). Of further note, mRNA expression of CEBPB was identified in the coronoid process, the condyle and the mandibular angle (Fig. 2a,b).
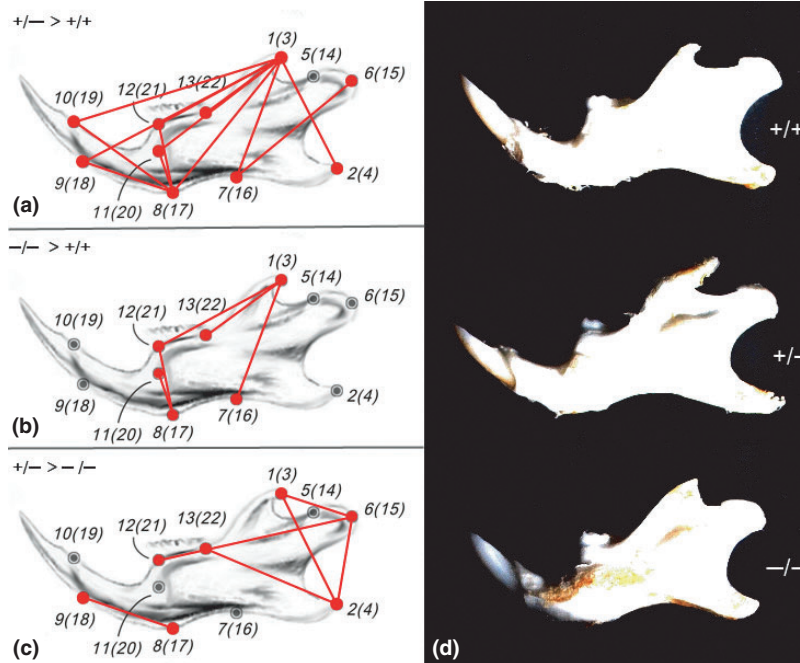
Figure 1 Difference in the mandibular morphology amongst CEBPB$^{+/-}$, CEBPB$^{-/-}$ and CEBPB$^{+/+}$ 12-month-old mice in this sample. (**a–c**) The schematic lateral view of the murine mandible and the landmark labels in the background were quoted from Richtsmeier *et al*, 2000 (License for the reuse received; License Number: 2784470273434). For bilateral landmarks, the number of the contralateral landmark is shown in parentheses. Landmark labels: 1(3), coronoid process; 2(4), mandibular angle; 5(14), anterior-most point on mandibular condyle; 6(15), posterior-most point on mandibular condyle; 7(16), superior-most point on inferior border of mandibular ramus (joining of angular notch with corpus); 8(17), inferior-most point on border of ramus inferior to incisor alveolar; 9(18), inferior-most point on incisor alveolar rim (at bone-tooth junction); 10(19), superior-most point on incisor alveolar rim (at bonetooth junction); 11(20), mental foramen; 12(21), anterior point on molar alveolar rim; 13(22), intersection of molar alveolar rim and base of coronoid process. Red lines illustrated the Euclidean distance matrix analysis (EDMA) linear distances that were (**a**) larger in CEBPB$^{+/-}$ mice compared to CEBPB$^{+/+}$ mice ($P < 0.05$), (**b**) larger in CEBPB$^{-/-}$ mice compared to CEBPB$^{+/+}$ mice ($P < 0.05$) and (**c**) larger in CEBPB$^{+/-}$ mice compared to CEBPB$^{-/-}$ mice ($P < 0.05$). (**d**) The photographic image showed a lateral view of three dry mandibles respectively collected from a CEBPB$^{+/+}$, a CEBPB$^{+/-}$ and a CEBPB$^{-/-}$ 12-month-old mice. Elongation of the coronoid process in CEBPB$^{+/-}$ and CEBPB$^{-/-}$ mice was confirmed by the morphology of the dry mandibles.

Table 1 Euclidean distance matrix analysis (EDMA) linear distances with significant difference between $CEBPB^{+/-}$ and $CEBPB^{+/+}$ 12-month-old mice ($n = 16$)

End-point Landmarks of EDMA Linear Distance		EDMA linear distance[a]		t-Statistic[b]	P-value
		$CEBPB^{+/-}$	$CEBPB^{+/+}$		
1: coronoid process	2: mandibular angle	6.05 ± 0.23	5.77 ± 0.24	−2.26	0.040
	7: superior-most point on inferior border of mandibular ramus	5.04 ± 0.21	4.63 ± 0.24	−3.68	0.002
	8: inferior-most point on border of ramus inferior to incisor alveolar	7.08 ± 0.31	6.76 ± 0.25	−2.19	0.046
	9: inferior-most point on incisor alveolar rim	8.74 ± 0.30	8.21 ± 0.34	−3.22	0.006
	10: superior-most point on incisor alveolar rim	8.73 ± 0.30	8.16 ± 0.31	−3.56	0.003
	11: mental foramen	6.64 ± 0.25	6.18 ± 0.27	−3.45	0.004
	12: anterior point on molar alveolar rim	5.28 ± 0.22	4.93 ± 0.22	−3.06	0.008
	13: intersection of molar alveolar rim and base of coronoid process	3.85 ± 0.21	3.53 ± 0.20	−2.92	0.011
6: posterior-most point on mandibular condyle	7: superior-most point on inferior border of mandibular ramus	5.89 ± 0.34	5.50 ± 0.27	−2.34	0.034
8: inferior-most point on border of ramus inferior to incisor alveolar	9: inferior-most point on incisor alveolar rim	3.24 ± 0.27	2.85 ± 0.20	−3.07	0.008
	10: superior-most point on incisor alveolar rim	4.48 ± 0.36	4.15 ± 0.05	−2.84	0.018
	11: mental foramen	1.88 ± 0.18	1.64 ± 0.09	−3.02	0.009
	12: anterior point on molar alveolar rim	3.30 ± 0.18	3.06 ± 0.03	−3.99	0.003
10: superior-most point on incisor alveolar rim	12: anterior point on molar alveolar rim	3.51 ± 0.16	3.32 ± 0.18	−2.18	0.047

[a]Mean ± standard deviation, under the micro-CT condition of 34 kilovolts (kV) and 39 microamperes (μA), with a source image receptor distance (SID) at 332.31 millimetres (mm) and a source object distance (SOD) at 180.43 mm.
[b]Statistical outcomes of the independent sample *t*-test.

Table 2 Euclidean distance matrix analysis (EDMA) linear distances with significant difference between $CEBPB^{-/-}$ and $CEBPB^{+/+}$ 12-month-old mice ($n = 12$)

End-point Landmarks of EDMA Linear Distance		EDMA Linear Distance[a]		t-Statistic[b]	P-value
		$CEBPB^{-/-}$	$CEBPB^{+/+}$		
1: coronoid process	7: superior-most point on inferior border of mandibular ramus	5.06 ± 0.32	4.63 ± 0.24	−2.63	0.025
	12: anterior point on molar alveolar rim	5.25 ± 0.18	4.93 ± 0.22	−2.72	0.021
	13: intersection of molar alveolar rim and base of coronoid process	3.91 ± 0.29	3.53 ± 0.20	−2.56	0.028
8: inferior-most point on border of ramus inferior to incisor alveolar	11: mental foramen	1.83 ± 0.13	1.64 ± 0.09	−2.80	0.019
	12: anterior point on molar alveolar rim	3.39 ± 0.29	3.06 ± 0.03	−2.80	0.019

[a]Mean ± standard deviation, under the micro-CT condition of 34 kV and 39 μA, with a SID at 332.31 mm and a SOD at 180.43 mm.
[b]Statistical outcomes of the independent sample *t*-test.

Table 3 Euclidean distance matrix analysis (EDMA) linear distances with significant difference between $CEBPB^{-/-}$ and $CEBPB^{+/-}$ 12-month-old mice ($n = 16$)

End-point Landmarks of EDMA Linear Distance		EDMA Linear Distance[a]		t-Statistic[b]	P-value
		$CEBPB^{-/-}$	$CEBPB^{+/-}$		
1: coronoid process	2: mandibular angle	5.68 ± 0.15	6.05 ± 0.23	3.42	0.004
	6: posterior-most point on mandibular condyle	3.27 ± 0.07	3.53 ± 0.25	2.43	0.029
2: mandibular angle	6: posterior-most point on mandibular condyle	3.64 ± 0.24	4.02 ± 0.23	3.14	0.007
	13: intersection of molar alveolar rim and base of coronoid process	5.39 ± 0.27	5.81 ± 0.41	2.24	0.042
6: posterior-most point on mandibular condyle	12: anterior point on molar alveolar rim	7.56 ± 0.22	7.90 ± 0.32	2.22	0.044
8: inferior-most point on border of ramus inferior to incisor alveolar	9: inferior-most point on incisor alveolar rim	2.82 ± 0.38	3.24 ± 0.27	2.56	0.023

[a]Mean ± standard deviation, under the micro-CT condition of 34 kV and 39 μA, with a SID at 332.31 mm and a SOD at 180.43 mm.
[b]Statistical outcomes of the independent sample *t*-test.
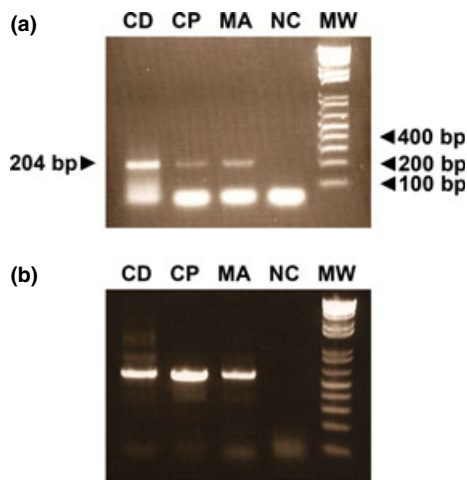
Figure 2 Assessment of mRNA expression in the condyle (CD), the coronoid process (CP), the mandibular angle (MA) and a negative control (NC) with a RT-PCR technique. The size of the molecular weight markers (MW) is displayed on the right, which is given in base pairs (bp). (**a**) CEBPB expression was identified in CD, CP and MA of a CEBPB$^{+/+}$ adult mouse. (**b**) GAPDH, as an internal control, was detected in the same sites of the mouse.

On the other hand, four (66.7%) of the six CEBPB$^{-/-}$ 12-month-olds sustained supernumerary teeth and/or odontomas in the diastema between the incisor and the first molar ($\chi^2 = 6.00$, df = 1, $P = 0.014$). Two supernumerary teeth accompanied with a complex odontoma near the root of the upper right incisor were identified in a CEBPB$^{-/-}$ adult (Fig. 3a–f), whilst two other CEBPB$^{-/-}$ mice simply showed a supernumerary tooth in the upper left quadrant. Another CEBPB$^{-/-}$ adult mouse did not display any supernumerary teeth in either jaw but an odontoma in the lower-right quadrant. All of the CEBPB$^{-/-}$ adults appeared with a normal number of erupted incisors and molars. Nevertheless, two (20%) of the ten CEBPB$^{+/-}$ 12-month-olds had a missing lower third molar ($\chi^2 = 1.37$, df = 1, $P = 0.242$). Dental anomalies such as supernumerary teeth, odontomas or hypodontia were not found in mice of any other genotypes and/or age.

Discussion

This study has demonstrated for the first time an enhancing effect of CEBPB homozygous deficiency on formation of supernumerary teeth. As odontomas have been deemed a type of supernumerary teeth (Howard, 1967) and all of the CEBPB$^{-/-}$ mice in this sample had a normal number of erupted teeth, the odontomas identified were added to the cases of supernumerary teeth. This contributed to the prevalence of supernumerary teeth as high as 66.7% amongst CEBPB nullizygotes. As RUNX2 deficiency is associated with hyperdontia (D'Souza *et al*, 1999) and CEBPB is involved in the positive regulation of both RUNX2 expression and activity (Gutierrez *et al*, 2002; Wiper-Bergeron *et al*, 2007; Lin *et al*, 2010), the discovery of supernumerary teeth in CEBPB$^{-/-}$ mice implied a potential role of CEBPB in regulating RUNX2 during odontogenesis as

well. On the other hand, in the prospective toothless diastema of murine jaws, extra tooth primordia normally developed and then underwent apoptosis to disappear within 24 h (Peterková *et al*, 2003). However, the supernumerary teeth of CEBPB$^{-/-}$ mice were exclusively observed in this gap. Because attenuated apoptosis was a consequence of CEBPB deficiency (Zinszner *et al*, 1998), the dental phenotype of CEBPB nullizygotes could also result from unsuccessful apoptosis of extra tooth primordia. Future investigations in the role of CEBPB on RUNX2 expression and apoptosis during tooth formation are indicated.

In addition, this study has reported a relationship between CEBPB deficiency and elongation of the coronoid process. The degree of elongation was most significant amongst CEBPB$^{+/-}$ mice, followed by CEBPB$^{-/-}$ mice. The CEBPB expression identified in the coronoid process confirmed the link between this mandibular phenotype and the genotypes. Since past studies suggested a negative effect of CEBPB on osteogenesis and chondrogenesis (Savage *et al*, 2006; Wiper-Bergeron *et al*, 2007; Hirata *et al*, 2009), an insufficient CEBPB function could impair the negative regulatory function, which was originally relevant to growth control of the coronoid process. However, this theory alone failed to explain the reason why other portions of the mandible were less affected than the coronoid process.

This phenomenon may be clarified by conceptualising the development of the temporomandibular joint. In humans, a secondary cartilaginous growth centre located at the coronoid process ordinarily disappears around birth (Dibbets, 1990), whilst in mice, formation of this secondary cartilage was suppressed except for a transient appearance on the 7th day after birth (Shibata *et al*, 2003). Failure to suppress the formation of the secondary cartilage led to an abnormal size and morphology of the coronoid process (Shibata *et al*, 2003). As morphological abnormalities of the mandible were not seen by the 14th day after birth in this sample, the attenuated apoptosis in virtue of CEBPB insufficiency (Zinszner *et al*, 1998) could prolong the survival of the secondary cartilage and consequently result in overgrowth of the coronoid process. Of further note, another secondary cartilaginous growth centre that normally vanishes around birth is located at the gonial area of the mandible (Dibbets, 1990). Expression of CEBPB has been confirmed in the mandibular angle as well. As this study has also reported longer EDMA line segments originating from the inferior border of the mandibular ramus in adult mice with CEBPB deficiency, findings related to the anatomical landmark coincided with the potentially delayed disappearance of the secondary cartilages.

Although both CEBPB$^{+/-}$ and CEBPB$^{-/-}$ mice demonstrated a lengthened coronoid process, this study identified a more significant elongation of this bony eminence in the former genotype. The suppressed differentiation of osteoblasts and the accordingly delayed bone formation owing to a complete loss of CEBPB (Tominaga *et al*, 2008) might lessen the overgrowth potential of the coronoid process. This concurred with
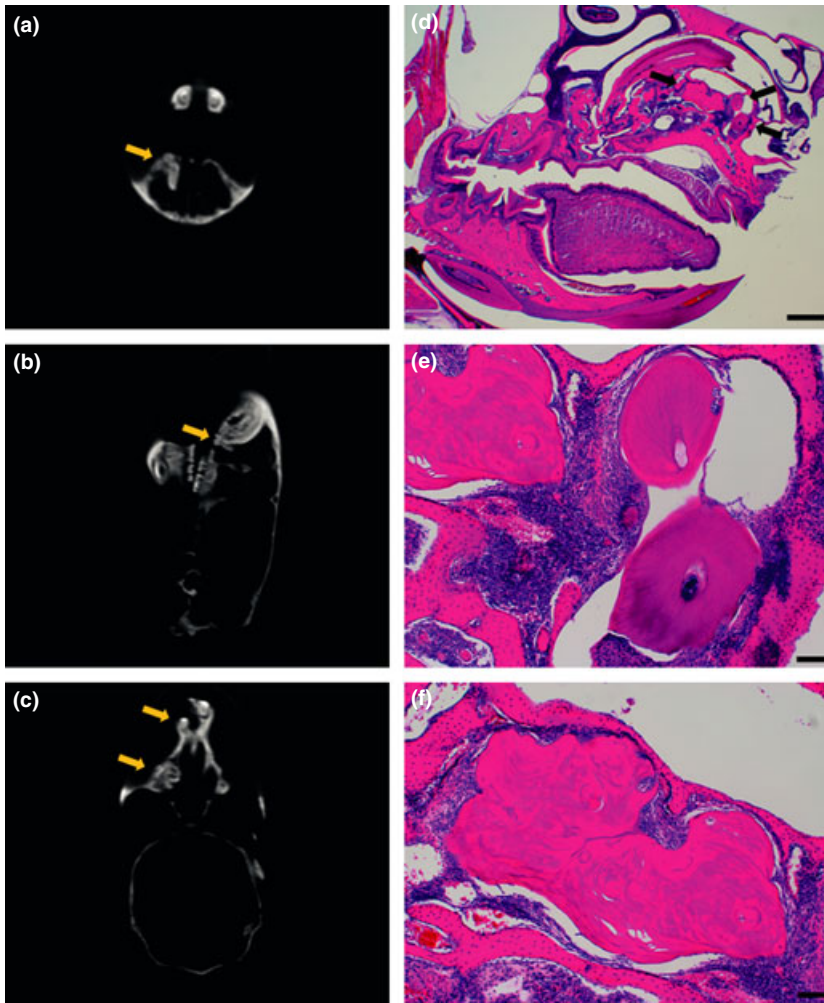
Figure 3 Dental anomalies identified in a CEBPB$^{-/-}$ 12-month-old mouse. (**a–c**) Micro-CT images of the murine head. (**a**) A frontal view displayed a tooth-like radiopaque object in the upper right quadrant (arrow). (**b**) A sagittal view showed two tooth-like radiopaque objects near the root of an incisor (arrow). (**c**) A transverse view exhibited asymmetry of the upper dentition (arrows). (**d–f**) Tissue photomicrographs of the murine head, in haematoxylin and eosin staining (HE stain). Depth of the tissue section: 880 μm inward from the most buccal point at the anatomic crown of the upper right first molar (5 μm per section). (**d**) Two supernumerary teeth and an odontoma were observed near the root of the upper right incisor (arrows). Scale bar: 1000 μm. (**e**) The pulp chamber and dentinal tubules of the supernumerary teeth were clearly seen in the enlarged view. Scale bar: 100 μm. (**f**) A well-defined border and various haphazardly arranged dental tissues of the tumour suggested a complex odontoma. Scale bar: 100 μm.

the observed difference in the condyle and the mandibular angle between CEBPB$^{+/-}$ and CEBPB$^{-/-}$ adult mice. To elucidate mechanisms for elongation of the coronoid process under CEBPB deficiency, further investigations are required.

Two CEBPB$^{+/-}$ adult mice had a missing lower third molar in spite of the lack of statistical significance. As the animals were killed at 12 months of age and this trait was not seen in younger mice, it is challenge to judge whether the missing teeth were owing to congenital agenesis or an acquired reason. A previous study has reported a connection between human hypodontia and an increase in RUNX2 dose (Mefford et al, 2010). As CEBPB could also act as a negative regulator of RUNX2 expression (Wiper-Bergeron et al, 2007), CEBPB heterozygosity might raise the dose of RUNX2 during tooth development and consequently contributed to dental agenesis. Of further note, hyperdontia and hypodontia have been separately observed in mice of different doses of ectodysplasin A receptor (EDAR) (Tucker et al, 2004). This inspired a possibility of dose dependency in tooth phenotypes of CEBPB as well. To prove the conjecture, future research with sufficient sample size and gene-dose quantification is needed.

Conclusions

This study has manifested that CEBPB deficiency is characterised by elongation of the coronoid process. Formation of supernumerary teeth in the diastema of CEBPB null mice has also been identified. In addition, the mandibular and dental phenotypes were unseen by the 14th day after birth.

CEBPB has been suggested as a regulator for various genes during osteogenesis and odontogenesis. The mandibular and dental phenotypes of CEBPB deficiency reported by this study could provide inspiration to tooth regeneration and/or aetiology of craniofacial deformity. Succeeding investigations into the influence of CEBPB on RUNX2 expression and apoptosis during mandibular and dental development are indicated.

the paper is indebted to Dr Maria Hui, Dr Kazumasa Nakao and Dr Noriaki Koyama for helpful discussions. Special thanks to Dr Mei-lan Chen and Dr Ahmed Hussain for their assistance in preparation of electronic artwork.

References

Altman DG, editor (1990). *Practical statistics for medical research*, 1st edn. Chapman and Hall/CRC: London.

Bai T, Tanaka T, Yukawa K, Umesaki N, Matsumoto M, Akira S (2006). Impaired postnatal development in C/EBPβ-deficient mice. *J Reprod Dev* **52:** 645–649.

Barbosa AC, Funato N, Chapman S *et al* (2007). Hand transcription factors cooperatively regulate development of the distal midline mesenchyme. *Dev Biol* **310:** 154–168.

Campbell R, Weinshel R, Backeljauw P, Wilson S, Bean J, Shao M (2009). Dental development in children with growth hormone insensitivity syndrome: Demirjian analysis of serial panoramic radiographs. *Cleft Palate Craniofac J* **46:** 409–414.

Cook MJ (1965). *The anatomy of the laboratory mouse*, 1st edn. Academic Press: New York.

Dibbets JMH (1990). Introduction to the temporomandibular joint. In: Enlow DH, ed *Facial growth*. Saunders: Philadelphia, pp. 149–163.

D'Souza RN, Aberg T, Gaikwad J *et al* (1999). Cbfa1 is required for epithelial-mesenchymal interactions regulating tooth development in mice. *Development* **126:** 2911–2920.

Gutierrez S, Javed A, Tennant DK *et al* (2002). CCAAT/enhancer-binding proteins (C/EBP) β and δ activate osteocalcin gene transcription and synergize with Runx2 at the C/EBP element to regulate bone-specific expression. *J Biol Chem* **277:** 1316–1323.

Harrison JR, Huang YF, Wilson KA *et al* (2005). Col1a1 promoter-targeted expression of p20 CCAAT enhancer-binding protein beta (C/EBPβ), a truncated C/EBPβ isoform, causes osteopenia in transgenic mice. *J Biol Chem* **280:** 8117–8124.

Hendricks-Taylor LR, Bachinski LL, Siciliano MJ *et al* (1992). The CCAAT/enhancer binding protein (C/EBPα) gene (CEBPA) maps to human chromosome 19q13.1 and the related nuclear factor NF-IL6 (C/EBPβ) gene (CEBPB) maps to human chromosome 20q13.1. *Genomics* **14:** 12–17.

Hirata M, Kugimiya F, Fukai A *et al* (2009). C/EBPβ Promotes transition from proliferation to hypertrophic differentiation of chondrocytes through transactivation of p57^{Kip2}. *PLoS ONE* **4:** e4543.

Howard RD (1967). The unerupted incisor. A study of the postoperative eruptive history of incisors delayed in their eruption by supernumerary teeth. *Dent Pract Dent Rec* **17:** 332–341.

Kawagishi H, Wakoh T, Uno H *et al* (2008). Hzf regulates adipogenesis through translational control of C/EBPα. *EMBO J* **27:** 1481–1490.

Kim JW, Hu JC, Lee JI *et al* (2005). Mutational hot spot in the DSPP gene causing dentinogenesis imperfecta type II. *Hum Genet* **116:** 186–191.

Lele S (1993). Euclidean distance matrix analysis (EDMA): estimation of mean form and mean form difference. *Math Geol* **25:** 573–602.

Lin KL, Chou CH, Hsieh SC, Hwa SY, Lee MT, Wang FF (2010). Transcriptional upregulation of DDR2 by ATF4 facilitates osteoblastic differentiation through p38 MAPK-mediated Runx2 activation. *J Bone Miner Res* **25:** 2489–2503.

McCarthy TL, Ji C, Chen Y, Kim K, Centrella M (2000). Time- and dose-related interactions between glucocorticoid and cyclic adenosine 3′,5′-monophosphate on CCAAT/enhancer-binding protein-dependent insulin-like growth factor I expression by osteoblasts. *Endocrinology* **141:** 127–137.

Mefford HC, Shafer N, Antonacci F *et al* (2010). Copy number variation analysis in single-suture craniosynostosis: multiple rare variants including RUNX2 duplication in two cousins with metopic craniosynostosis. *Am J Med Genet A* **152A:** 2203–2210.

Narayanan K, Ramachandran A, Peterson MC *et al* (2004). The CCAAT enhancer-binding protein (C/EBP)β and Nrf1 interact to regulate dentin sialophosphoprotein (DSPP) gene expression during odontoblast differentiation. *J Biol Chem* **279:** 45423–45432.

Peterková R, Peterka M, Lesot H (2003). The developing mouse dentition: a new tool for apoptosis study. *Ann N Y Acad Sci* **1010:** 453–466.

Poli V (1998). The role of C/EBP isoforms in the control of inflammatory and native immunity functions. *J Biol Chem* **273:** 29279–29282.

Richtsmeier JT, Baxter LL, Reeves RH (2000). Parallels of craniofacial maldevelopment in Down syndrome and Ts65Dn mice. *Dev Dyn* **217:** 137–145.

Salmela E, Alaluusua S, Sahlberg C, Lukinmaa PL (2012). Tributyltin alters osteocalcin, matrix metalloproteinase 20 and dentin sialophosphoprotein gene expression in mineralizing mouse embryonic tooth in vitro. *Cells Tissues Organs* **195:** 287–295.

Savage T, Bennett T, Huang YF *et al* (2006). Mandibular phenotype of p20C/EBPβ transgenic mice: reduced alveolar bone mass and site-specific dentin dysplasia. *Bone* **39:** 552–564.

Seagroves TN, Krnacik S, Raught B *et al* (1998). C/EBPβ, but not C/EBPα, is essential for ductal morphogenesis, lobuloalveolar proliferation, and functional differentiation in the mouse mammary gland. *Genes Dev* **12:** 1917–1928.

Shibata S, Suda N, Fukada K, Ohyama K, Yamashita Y, Hammond VE (2003). Mandibular coronoid process in parathyroid hormone-related protein-deficient mice shows ectopic cartilage formation accompanied by abnormal bone modeling. *Anat Embryol (Berl)* **207:** 35–44.

Suzuki T, Higgins PJ, Crawford DR (2000). Control selection for RNA quantitation. *Biotechniques* **29:** 332–337.

Tanaka T, Akira S, Yoshida K *et al* (1995). argeted disruption of the NF-IL6 gene discloses its essential role in bacteria killing and tumor cytotoxicity by macrophages. *Cell* **80:** 353–361.

Tominaga H, Maeda S, Hayashi M *et al* (2008). CCAAT/enhancer-binding protein β promotes osteoblast differentiation by enhancing Runx2 activity with ATF4. *Mol Biol Cell* **19:** 5373–5386.

Tucker AS, Headon DJ, Courtney JM, Overbeek P, Sharpe PT (2004). The activation level of the TNF family receptor, Edar, determines cusp number and tooth number during tooth development. *Dev Biol* **268:** 185–194.

Wiper-Bergeron N, St-Louis C, Lee JM (2007). CCAAT/Enhancer binding protein β abrogates retinoic acid-induced osteoblast differentiation via repression of Runx2 transcription. *Mol Endocrinol* **21:** 2124–2135.

Wolterink-Donselaar IG, Meerding JM, Fernandes C (2009). A method for gender determination in newborn dark pigmented mice. *Lab Anim (NY)* **38:** 35–38.

Zinszner H, Kuroda M, Wang X *et al* (1998). CHOP is implicated in programmed cell death in response to impaired function of the endoplasmic reticulum. *Genes Dev* **12:** 982–995.